Mutual Coupling Exploitation for Point-to-point MIMO by Constructive Interference

Ang Li and Christos Masouros
Dept. of Electronic and Electrical Eng., University College London, London, UK
Email: {ang.li.14, c.masouros}@ucl.ac.uk

***Abstract*—In this paper, we propose a joint analog-digital (A/D) beamforming scheme for the point-to-point (P2P) multiple-input-multiple-output (MIMO) systems, where we exploit the mutual coupling effect to further improve the system performance. By judiciously selecting the value of each load impedance for the antenna array, it will be shown that the mutual coupling effect can be beneficial. We firstly prove that the full elimination of mutual coupling is not achievable solely by changing the values of each load impedance. We further propose a joint A/D technique where the resulting interference aligns constructively to the useful signal vector with the concept of constructive interference. Numerical results show that the proposed schemes can achieve an improved performance compared to systems with fixed mutual coupling, especially when the antenna spacing is small.**

***Index Terms*—MIMO, mutual coupling, constructive interference, optimization.**

I. Introduction

Due to the significant performance gains over conventional single-input-single-output (SISO) systems, multiple-input-multiple-output (MIMO) systems have been widely studied in recent years. Among MIMO techniques, one of the most popular applications is to employ spatial multiplexing to improve the system capacity by sending parallel data streams over multiple antennas [1][2]. These data streams can be successfully decoded at the receiver by equalization techniques. Among receiver architectures, the maximum likelihood (ML) receiver can achieve the optimal performance, while the high complexity hinders its application for practical scenarios [3]. Therefore, linear receivers such as zero-forcing (ZF) and minimum mean-squared-error (MMSE) that can offer a sub-optimal performance are proposed as alternative techniques [4][5]. The successive interference cancellation (SIC) scheme proposed in [6] can further improve the detection performance, with an increased computational complexity. Due to the low complexity, linear receivers are more promising for many applications than the optimal ML receiver.

Many existing studies on the receiver structures assume an uncorrelated Rayleigh flat fading channel, where no spatial correlation or mutual coupling (MC) among antenna elements is considered. Nevertheless, when the spacing between antenna elements is small, these two effects have a significant impact on the system performance and should not be neglected [7][8]. Therefore, studies have been conducted on the correlation and MC. In [9]-[11], the effect of spatial correlation is studied for MIMO systems, where the channel model with spatial correlation is derived. Experimental studies on the effect of transmit correlation have been conducted in [12]-[14], and the impact on the MIMO system performance has been studied in [15]-[17]. Based on these studies, several designs of the robust pre-processing techniques are proposed in [18]-[20].

For the study of the MC effect, in [21] it is shown that the effect of MC can be characterized by a coupling matrix, based on which the impact of MC on MIMO capacity is studied. Further studies on the MC can be found in [22]-[25], where in [22] the MC is studied in a Rician channel for transmit beamforming. It is shown that when the line-of-sight (LOS) component of the channel is dominant, the system can achieve an improved capacity. [24] studies the MC for MIMO systems and shows that MC has an impact on the system performance, and this impact can be more significant when the antenna spacing is small. In [25], the effect of MC is studied for MIMO systems at high SNR, where it is shown that for low correlated propagation environments, the MC effect will degrade the system performance.

To compensate for the performance loss introduced by the MC effect, a number of techniques have been proposed, which focus on suppressing the performance degradation by deriving a compensation matrix [26][27]. Some novel structures are also proposed to eliminate the MC effect. For example, in [28], a mantle cloaking method is applied to strip dipole antenna arrays to reduce the mutual coupling effect at low-terahertz (THz) frequencies. In [29], a U-shaped microstrip is introduced to suppress the mutual coupling effect. Parasitic elements are introduced in [30] to formulate a reverse coupling to alleviate the effect of mutual coupling. Other approaches targeting at MC suppression can be found in [31]-[33].

In this paper, we propose to exploit the MC effect rather than suppressing or eliminating this effect, to further improve the point-to-point (P2P) MIMO detection performance. In the proposed scheme, each antenna element is equipped with a tunable load impedance (for example varactors) such that the MC effect can be controlled by tuning each load impedance. While it will be shown that the full elimination of MC is not achievable, with tunable loads we can exploit the concept of constructive interference to further achieve an improved performance. By judiciously selecting each value of the load impedances, the resulting MC matrix can be constructive and lead to a better detection performance, where each resulting symbol is strictly aligned to the phase of the original symbol with an enhancement in the transmit power. The problem is formulated into a convex optimization problem and the

practical constraint is also considered, where a look-up table can be built such that the proposed techniques can be efficiently applied. In this paper we focus on P2P links where typically small scale MIMO systems are considered, such as the device-to-device (D2D) communications and small-cells that have received increasing research attention recently and will play an indispensable role in the future communication standards. The proposed schemes are then best suited to these scenarios, with a relatively small number of antennas at both the transmitter and the receiver, where the size of the look-up table is acceptable, and the interference is present and can be exploited. The simulation results validate the performance advantages of the proposed schemes.

$Notations$: a, $\mathbf{a}$, and $\mathbf{A}$ denote scalar, vector and matrix, respectively. $(\cdot)^T$, $(\cdot)^H$, $(\cdot)^{-1}$, $(\cdot)^\dagger$, and $tr(\cdot)$ denote transpose, conjugate transpose, inverse, Moore-Penrose inverse and trace of a matrix respectively. $\mathbf{I}$ is the identity matrix and $\mathbf{0}$ denotes a zero matrix or vector. $\mathcal{C}^{n\times n}$ represents $n \times n$ matrix in the complex set. $diag(\cdot)$ denotes the conversion of a vector into a diagonal matrix with the values on its main diagonal and $vec(\cdot)$ is the operation of transforming a diagonal matrix into a column vector. $\Re(\cdot)$ and $\Im(\cdot)$ denote the real part and imaginary part of a complex number, respectively.

II. System Model

We consider a P2P MIMO system with N_t transmit antennas and N_r receive antennas where $N_t \leq N_r$. The $N_t \times 1$-dimensional transmit symbol vector is firstly multiplied by a MC matrix $\mathbf{Z}_t \in \mathcal{C}^{N_t\times N_t}$ before transmission and then a receiving MC matrix $\mathbf{Z}_r \in \mathcal{C}^{N_r\times N_r}$ at the receiver side. The received signal vector can therefore be obtained as

$$\mathbf{y} = \mathbf{Z}_r\mathbf{H}\mathbf{Z}_t\mathbf{s} + \mathbf{w}, \tag{1}$$

where $\mathbf{s} \in \mathcal{C}^{N_t\times 1}$ denotes the transmit symbol vector from a normalized PSK modulation and for each symbol $\|s_i\|^2 = 1$, $\forall i \in \{1, 2, ..., N_t\}$. $\mathbf{H} \in \mathcal{C}^{N_r\times N_t}$ is the channel matrix, and $\mathbf{w}$ is the additive white Gaussian noise (AWGN) vector where we assume $\mathbf{w} \sim \mathcal{CN}\left(\mathbf{0}, \sigma^2 \cdot \mathbf{I}\right)$. As we focus on the signal processing approaches at the transmitter, the MC at the transmitter side is considered while we assume $\mathbf{Z}_r = \mathbf{I}$, which is in line with the studies of the MC effect in [26]-[30]. We note that the proposed schemes can be trivially applied to $\mathbf{Z}_r \neq \mathbf{I}$ by considering the effective channel $\hat{\mathbf{H}} = \mathbf{Z}_r\mathbf{H}$. At the receiver, the signal vector is filtered by a channel-dependent equalizer $\mathbf{G} \in \mathcal{C}^{N_t\times N_r}$, and the signal vector for demodulation can be obtained as

$$\mathbf{r} = \mathbf{G}\mathbf{y} = \mathbf{G}\mathbf{H}\mathbf{Z}_t\mathbf{s} + \mathbf{G}\mathbf{w}. \tag{2}$$

A. Channel Model

When the spacing between the adjacent antenna elements is small, the spatial correlation effect becomes significant and should be characterized in the channel model. For a P2P MIMO system, as considered in this paper, there exist correlation effects at both the transmit side and receive side. Therefore, a fully correlated non-line-of-sight (NLOS) geometric Rayleigh flat fading channel is assumed, which can be modeled as [9]-[11]

$$\mathbf{H} = \mathbf{A}_r\mathbf{H}_N\mathbf{A}_t^H. \tag{3}$$

In (3), $\mathbf{H}_N \in \mathcal{C}^{N\times N}$ is diagonal and can be expressed as

$$\mathbf{H}_N = \frac{1}{\sqrt{N}} \cdot diag(h_1, h_2, ..., h_N), \tag{4}$$

where N is the number of random and independent paths [9]. h_i, $\forall i \in \{1, 2, ..., N\}$ is the complex Rayleigh channel coefficient and $h_i \sim \mathcal{CN}(0, 1)$. $\mathbf{A}_r \in \mathcal{C}^{N_r\times N}$ and $\mathbf{A}_t \in \mathcal{C}^{N_t\times N}$ denote the receiver-side and transmitter-side steering matrices that contain N steering vectors of the antenna array, which characterize the correlation effect. For uniform linear arrays (ULAs), as assumed in this paper, $\mathbf{A}_r$ and $\mathbf{A}_t$ can be expressed as

$$\begin{aligned}\mathbf{A}_r &= [\mathbf{a}_r(\alpha_1), \mathbf{a}_r(\alpha_2), ..., \mathbf{a}_r(\alpha_N)],\\ \mathbf{A}_t &= [\mathbf{a}_t(\beta_1), \mathbf{a}_t(\beta_2), ..., \mathbf{a}_t(\beta_N)],\end{aligned} \tag{5}$$

where $\mathbf{a}_r(\alpha_i) \in C^{N_r\times 1}$ and $\mathbf{a}_t(\beta_i) \in C^{N_t\times 1}$ of ULAs can be expressed as

$$\begin{aligned}\mathbf{a}_r(\alpha_i) &= \left[1, e^{j2\pi d_r \sin\alpha_i}, ..., e^{j2\pi(N_r-1)d_r\sin\alpha_i}\right]^T,\\ \mathbf{a}_t(\beta_i) &= \left[1, e^{j2\pi d_t \sin\beta_i}, ..., e^{j2\pi(N_t-1)d_t\sin\beta_i}\right]^T.\end{aligned} \tag{6}$$

α_i and β_i denote the angles of arrival (AoAs) and angles of departure (AoDs) respectively, with the assumption that each α_i and β_i follow a uniform distribution in $[-\pi, \pi]$. d_r and d_t denote the antenna spacing normalized by the carrier wavelength for the receive and transmit antenna array, respectively.

B. Modeling of the Mutual Coupling

Based on [7][21][23], the MC matrix with tunable load impedances can be derived and obtained as

$$\mathbf{Z}_t(\mathbf{z}_L) = [z_A \cdot \mathbf{I} + diag(\mathbf{z}_L)]\,[\mathbf{\Gamma} + diag(\mathbf{z}_L)]^{-1}, \tag{7}$$

where z_A denotes the antenna impedance and $\mathbf{z}_L = \left[z_{L_1}, z_{L_2}, ..., z_{L_{N_t}}\right]^T$ is the load impedance vector to be optimized. $\mathbf{\Gamma}$ is the mutual impedance matrix which can be expressed as [21][23]

$$\mathbf{\Gamma} = \begin{bmatrix} z_A & z_{m_1} & z_{m_2} & \cdots & z_{m_{N_t-1}} \\ z_{m_1} & z_A & z_{m_1} & \ddots & \vdots \\ z_{m_2} & z_{m_1} & \ddots & \ddots & z_{m_2} \\ \vdots & \ddots & \ddots & \ddots & z_{m_1} \\ z_{m_{N_t-1}} & \cdots & z_{m_2} & z_{m_1} & z_A \end{bmatrix}. \tag{8}$$

where z_{m_k} denotes the mutual impedance of two antenna elements with an inter-spacing of kd_t. The value of z_A and z_{m_k} can be obtained by the induced electromagnetic-field (EMF) method [Chapter 8, 23] based on d_t.

III. Proposed Constructive Scheme

In this paper, when there exists MC effect at the transmitter, the transmit signal vector after MC can be expressed as

$$\widehat{\mathbf{s}} = \mathbf{Z}_t \mathbf{s}, \tag{9}$$

where there will be interference among the resulting data symbols if $\mathbf{Z}_t \neq \mathbf{I}$. Before the proposed scheme is introduced, by denoting $z_{x_i} = z_A + z_{L_i}$ we note that (7) can be equivalently expressed as

$$\mathbf{Z}_t = \mathbf{Z}_x [\mathbf{B} + \mathbf{Z}_x]^{-1}, \tag{10}$$

where $\mathbf{Z}_x = diag\left(z_{x_1}, z_{x_2}, ..., z_{x_{N_t}}\right)$ and $\mathbf{B} = \mathbf{\Gamma} - z_A \cdot \mathbf{I}$. From (9), the MC effect at the transmitter is fully characterized by the MC matrix multiplied to the transmit symbol vector, which can be regarded as a linear scaling effect to the data symbol $\mathbf{s}$, and (9) can be further expressed as

$$\widehat{\mathbf{s}} = \mathbf{Z}_t \mathbf{s} = \mathbf{Z}_x (\mathbf{B} + \mathbf{Z}_x)^{-1} \mathbf{s}. \tag{11}$$

It is known that the linear scaling effect of a matrix can be equivalently represented by the multiplication of a diagonal matrix, and therefore by introducing a diagonal matrix $diag\left(\mathbf{\Lambda}\right)$, (11) can be equivalently expressed as

$$\widehat{\mathbf{s}} = diag\left(\mathbf{\Lambda}\right) \mathbf{s}, \tag{12}$$

where $\mathbf{\Lambda} = [\lambda_1, \lambda_2, ..., \lambda_{N_t}]^T$ and λ_i is the scaling factor for transmit symbol s_i. The property of λ_i can then represent the MC effect for each transmit symbol. It should be noted that the expression of (12) is only a mathematical representation, and does not necessarily mean that there is no interference between transmit symbols because each λ_i can be a complex number. Then, based on (11) and (12), we can obtain

$$\mathbf{Z}_x (\mathbf{B} + \mathbf{Z}_x)^{-1} \mathbf{s} = diag\left(\mathbf{\Lambda}\right) \mathbf{s}, \tag{13}$$

which can be further transformed into

$$\begin{aligned} &\mathbf{s} = \left(\mathbf{B} + \mathbf{Z}_x\right) \mathbf{Z}_x^{-1} diag\left(\mathbf{\Lambda}\right) \mathbf{s} \\ \Rightarrow\ &\left[diag\left(\mathbf{\Lambda}\right) - \mathbf{I}\right] \mathbf{s} + \mathbf{B} \mathbf{Z}_x^{-1} diag\left(\mathbf{\Lambda}\right) \mathbf{s} = 0. \end{aligned} \tag{14}$$

We note that for practical antenna arrays, $\mathbf{B}$ and $\mathbf{Z}_x$ are both invertible, which enables the following designs.

A. Full Elimination of the Mutual Coupling

We firstly consider the approach on the full elimination of the MC matrix such that there is no performance loss, which means that $\widehat{\mathbf{s}} = \mathbf{s}$. According to (12), this is equivalent to

$$\lambda_i = 1, \ \ \forall i \in \{1, 2, ..., N_t\}. \tag{15}$$

Substituting (15) into (14) yields

$$\mathbf{B} \mathbf{Z}_x^{-1} \mathbf{s} = 0, \tag{16}$$

and (16) can be further transformed into

$$\mathbf{B} \cdot diag\left(\mathbf{s}\right) vec\left(\mathbf{Z}_x^{-1}\right) = 0, \tag{17}$$

which leads to the following proposition.

Proposition: It is not achievable to fully eliminate the MC effect by solely tuning the value of each load impedance.

Proof: Note that (17) means finding $\mathbf{Z}_x^{-1}$ to satisfy (17) for a specific transmit symbol vector $\mathbf{s}$. This is equivalent to finding a non-zero solution of the linear system $\mathbf{A}\mathbf{x} = 0$, where $\mathbf{A} = \mathbf{B} \cdot diag\left(\mathbf{s}\right)$ and $\mathbf{x} = vec\left(\mathbf{Z}_x^{-1}\right)$. Based on linear algebra theory, the condition for a non-zero solution for such a system is $\det\left(\mathbf{A}\right) = 0$, which means

$$\det\left[\mathbf{B} \cdot diag\left(\mathbf{s}\right)\right] = 0, \tag{18}$$

and (18) can be further obtained as

$$\det\left[\mathbf{B}\right] = 0 \ \ or \ \ \det\left[diag\left(\mathbf{s}\right)\right] = 0. \tag{19}$$

Noting that $\mathbf{B} = \mathbf{\Gamma} - z_A \cdot \mathbf{I}$ has a non-zero determinant and $\det\left[diag\left(\mathbf{s}\right)\right] \neq 0$, it is therefore not possible for (17) to have a non-zero solution, which proves the proposition. ■

B. Constructive Mutual Coupling Exploitation

Although the full elimination of MC solely by changing the values of each load impedance is not achievable, we can exploit the concept of constructive interference to rotate the angles of the interfering signals by selecting the value of each load impedance such that the resulting MC effect is constructive and further benefits the system performance. Constructive interference is defined as the interference that pushes the interfered symbols away from the detection thresholds. The concept of constructive interference is firstly exploited to further improve the performance of MIMO systems by precoding schemes in [34]-[36], where the angles of the interfering signals are controlled and rotated such that the interfering signals are strictly aligned to the phase of the desired symbol, which leads to a better detection performance. For the mutual coupling exploitation, we optimize each value of the load impedance such that the resulting MC matrix is constructive and improves the power of the transmit symbol vector. Based on (12), this is equivalent to

$$\lambda_i \geq 1, \ \ \forall i \in \{1, 2, ..., N_t\}, \tag{20}$$

where λ_i can be seen as a constructive coefficient. Recall (13) and with some transformations, we can obtain

$$\begin{aligned} &\mathbf{B} \mathbf{Z}_x^{-1} diag\left(\mathbf{\Lambda}\right) \mathbf{s} = \left[\mathbf{I} - diag\left(\mathbf{\Lambda}\right)\right] \mathbf{s} \\ \Rightarrow\ &vec\left(\mathbf{Z}_x^{-1}\right) = diag\left(\mathbf{\Omega}\right) \mathbf{B}^{-1} \left[\mathbf{I} - diag\left(\mathbf{\Lambda}\right)\right] \mathbf{s}, \end{aligned} \tag{21}$$

where $\mathbf{\Omega} = \left[\frac{1}{\lambda_1 s_1}, \frac{1}{\lambda_2 s_2}, ..., \frac{1}{\lambda_{N_t} s_{N_t}}\right]^T$. It can be observed that for a given symbol vector, we can obtain $vec\left(\mathbf{Z}_x^{-1}\right)$ with an arbitrary value of λ_i. However, the values of the resulting load impedances may be infeasible in practice, as the real part of the load impedance should be ensured positive such that the antenna array can radiate power [37][38]. Therefore in this paper, we employ convex optimization to obtain the optimal values of the load impedances under this practical implementation constraint, as detailed below.

As λ_i is the constructive coefficient for s_i which can be seen as a power enhancement factor, we therefore consider

a max-min optimization problem in which we maximize the minimum value of λ_i, expressed as

$$\begin{aligned}\mathcal{P}_0: \max_{z_{L_i}} \min \quad & \lambda_i \\ s.t. \quad & (\lambda_i - 1)\, s_i + \left[\mathbf{B}\mathbf{Z}_x^{-1} diag\left(\mathbf{\Lambda}\right)\mathbf{s}\right]_i = 0,\ \forall i \in \mathcal{I} \\ & \Re\left(z_{L_i}\right) \geq 0,\ \forall i \in \mathcal{I} \\ & \lambda_i \geq 1,\ \forall i \in \mathcal{I}\end{aligned} \tag{22}$$

where we denote $\mathcal{I} = \{1, 2, ..., N_t\}$ for simplicity. By denoting

$$t_i = \lambda_i - 1, \tag{23}$$

and

$$\mathbf{x} = \left[\frac{\lambda_1}{z_A + z_{L_1}}, \frac{\lambda_2}{z_A + z_{L_2}}, ..., \frac{\lambda_{N_t}}{z_A + z_{L_{N_t}}}\right]^T, \tag{24}$$

the max-min optimization in (22) can be further transformed into a max optimization problem, which is given by

$$\begin{aligned}\mathcal{P}_1: \max_{t_i, x_i} \quad & Q \\ s.t. \quad & t_i s_i + \left[\mathbf{B} diag\left(\mathbf{x}\right)\mathbf{s}\right]_i = 0,\ \forall i \in \mathcal{I} \\ & \Re\left(z_{L_i}\right) \geq 0,\ \forall i \in \mathcal{I} \\ & Q \leq t_i + 1,\ \forall i \in \mathcal{I} \\ & t_i \geq 0,\ \forall i \in \mathcal{I}\end{aligned} \tag{25}$$

where Q is an introduced variable. Based on (23)(24), the load impedance z_{L_i} can be obtained as

$$z_{L_i} = \frac{t_i + 1}{x_i} - z_A, \tag{26}$$

and the constraint that $\Re\left(z_{L_i}\right) \geq 0$ is equivalent to

$$\begin{aligned}\Re\left(\frac{t_i + 1}{x_i}\right) \geq \Re\left(z_A\right) \Rightarrow\ & \frac{\left(t_i + 1\right) \cdot \Re\left(x_i\right)}{\left|x_i\right|^2} \geq \Re\left(z_A\right) \\ \Rightarrow\ & \Re\left(x_i\right) \geq \frac{\Re\left(z_A\right)}{t_i + 1} \left|x_i\right|^2.\end{aligned} \tag{27}$$

Noting that (27) is a non-convex constraint and makes the optimization problem non-convex, we therefore relax this constraint into a convex one. Based on (20)(23) we note that $\left(t_i + 1\right) \geq 1$, therefore we have

$$\Re\left(z_A\right) \cdot \left|x_i\right|^2 \geq \frac{\Re\left(z_A\right)}{t_i + 1} \left|x_i\right|^2. \tag{28}$$

Then, if the following constraint is satisfied:

$$\Re\left(x_i\right) \geq \Re\left(z_A\right) \cdot \left|x_i\right|^2, \tag{29}$$

the constraint in (27) is also satisfied. We therefore employ the constraint in (29) to substitute the constraint in the optimization problem, and in this way the original problem is transformed into a convex optimization problem and can be efficiently solved. The final optimization problem can be formulated as

$$\begin{aligned}\mathcal{P}_2: \max_{t_i, x_i} \quad & Q \\ s.t. \quad & t_i s_i + \left[\mathbf{B} diag\left(\mathbf{x}\right)\mathbf{s}\right]_i = 0,\ \forall i \in \mathcal{I} \\ & \Re\left(x_i\right) \geq \Re\left(z_A\right) \cdot \left|x_i\right|^2,\ \forall i \in \mathcal{I} \\ & Q \leq t_i + 1,\ \forall i \in \mathcal{I} \\ & t_i \geq 0,\ \forall i \in \mathcal{I}\end{aligned} \tag{30}$$

(30) is a second-order cone programming (SOCP) and can be efficiently solved by convex optimization tools such as CVX and SeDuMi. Then, the optimal load impedance for each antenna element can be calculated based on (26).

IV. Practical Implementation

It can be observed from the above derivation that the optimal value of each load impedance is solely dependent on the transmit symbol vector, irrespective of the channel $\mathbf{H}$. Therefore, a look-up table can be built for the optimal values of each load impedance based on the transmit symbol vector. With this approach, the optimization process can be conducted offline to obtain the optimal values prior to the data transmission, and this information can then be kept for future data transmission, where a symbol-by-symbol optimization is no longer needed, which can significantly reduce the complexity. For D2D and small-cell scenarios where the number of antennas is relatively small at both the transmitter and the receiver, the proposed schemes can be efficiently applied by using the look-up table.

On the other hand, the equalizer $\mathbf{G}$ at the receiver requires the knowledge of $\mathbf{H}$, however with pilots we can only obtain $\tilde{\mathbf{H}} = \mathbf{H}\mathbf{Z}_t^0$ at the receiver. Therefore, the receiver needs to extract $\mathbf{H}$ from $\tilde{\mathbf{H}}$. We note that the mutual impedance $\mathbf{\Gamma}$ is only dependent on the array structure and does not change. Therefore $\mathbf{\Gamma}$ is typically known to the transmitter, either by the induced EMF method or other measurements, and further known to the receiver by forwarding. At the pilot stage the load impedance vector $\mathbf{z}_L$ is set to a specific value (for example 50Ω for each load impedance) known to the receiver, denoted as $\mathbf{z}_L^0$, and we further denote the resulting MC matrix as $\mathbf{Z}_t^0$. We then obtain $\tilde{\mathbf{H}} = \mathbf{H}\mathbf{Z}_t^0$, and as $\mathbf{Z}_t^0$ is known to the receiver, $\mathbf{H}$ can be extracted from $\tilde{\mathbf{H}}$ to obtain the equalizer $\mathbf{G}$.

Still, we note that the proposed scheme needs to tune the value of each load impedance based on the transmit symbol vector during data transmission. Therefore, technologies that support the frequent tuning of the load impedances are necessary, which has been proposed and studied in [39] and the references therein. It is shown that both semiconductor-based and ferroelectric-based varactors that can support a tuning speed as fast as 1-100 ns have been designed. Furthermore, recent studies on electronically steerable parasitic array radiators (ESPARs) have also supported the frequent tuning of the load impedances [40][41]. The successful proof-of-concept experiments and implementation of ESPARs have therefore motivated the design of the proposed schemes [42].

V. Numerical Results

In this section the numerical results based on Monte Carlo simulations are presented. We assume the system operates at the frequency $f = 2.6$GHz and QPSK modulation is employed. It should be noted that the extension to higher PSK is also applicable [34], and for QAM modulation the constructive interference can be exploited for the outer constellation points [35]. We consider a 4×4 P2P MIMO system, where the simulated channel is based on (3)-(6) and $N = 50$. As we assume $\mathbf{Z}_r = \mathbf{I}$ at the receiver side, in the simulations

$d_r = 0.5$. We focus on a compact array and the MC effect is more dominant when the antenna spacing is small, and therefore at the transmitter a dipole antenna array with $d_t = 0.2$ is assumed, while we also compare the performance with different values of the antenna spacing d_t. The above parameters remain the same throughout the simulations unless otherwise stated. For the receiver structure $\mathbf{G}$, we employ both ZF and MMSE receivers, which are expressed as

$$\begin{aligned} \mathbf{G}_{ZF} &= \left(\mathbf{H}^H\mathbf{H}\right)^{-1}\mathbf{H}^H, \\ \mathbf{G}_{MMSE} &= \left(\mathbf{H}^H\mathbf{H} + \frac{N_t}{\rho}\cdot\mathbf{I}\right)^{-1}\mathbf{H}^H, \end{aligned} \tag{31}$$

where $\rho = \frac{1}{\sigma^2}$ denotes the transmit SNR. We compare our results with the ML receiver and hard detection is performed after equalization.

In Fig. 1, the bit error rate (BER) performance of the proposed scheme is compared to conventional case with fixed mutual coupling (denoted as "with MC") and an ideal case where there is no mutual coupling effect (denoted as "no MC"). Note that the case "no MC" is only shown as a reference. The proposed scheme is denoted as "Constructive". It is seen that MMSE-based schemes outperform ZF-based schemes. Furthermore, for both ZF and MMSE, it can be observed that the proposed scheme outperforms the conventional case with fixed mutual coupling with an SNR gain over 5dB and even performs better than the case without mutual coupling, as the mutual coupling effect is exploited to further improve the system performance.

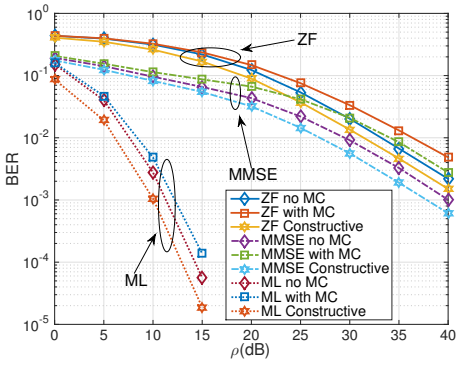

Fig. 1: BER v.s. SNR, d_t=0.2, d_r=0.5, QPSK

Fig. 2 presents the BER performance with respect to the normalized antenna spacing at the transmitter. For both schemes, the BER performance is improved with the increase in the antenna spacing, which is because of the reduced correlation effect. Moreover, it is important to observe that the performance gain of the proposed schemes becomes larger when the antenna spacing is small, due to the fact that the mutual coupling effect becomes stronger when the antenna spacing is small. This result means that the proposed schemes are more favourable with a small antenna spacing, which enables the design of compact antenna arrays.

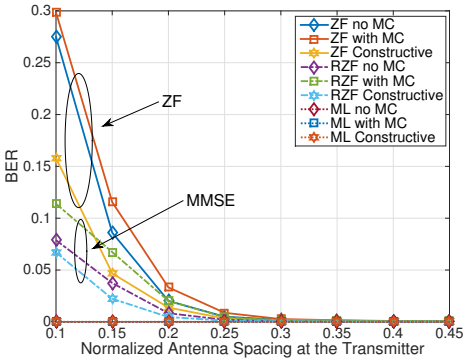

Fig. 2: BER v.s. transmit antenna spacing, SNR=30dB, d_r=0.5, QPSK

Noting that the proposed scheme is modulation dependent which makes the expression of Shannon capacity inaccurate, in Fig. 3 we therefore show the average throughput of ZF and MMSE based schemes to illustrate the capacity benefits, where the throughput is expressed as $T_r = (1 - \text{BLER}) \cdot m \cdot N_t \; bits/channel \; use$, where BLER is the block error rate and m=2 bit/symbol for QPSK. The block length is assumed to be 20 symbols. As can be seen, the proposed scheme achieves an improved performance on the average throughput for both ZF and MMSE receivers. MMSE achieves a better performance at low SNR compared to ZF, and achieves a similar performance when the SNR is high.

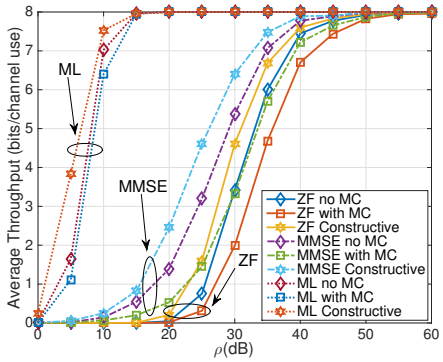

Fig. 3: Average throughput v.s. SNR, d_t=0.2, d_r=0.5, QPSK, Block length=20 symbols

VI. Conclusion

In this paper, we study the mutual coupling effect among MIMO antennas and further exploit this effect to benefit the MIMO performance. By solely changing the values of each load impedance, the mutual coupling effect can be controlled. We then propose a constructive mutual coupling exploitation technique to further improve the performance of MIMO, which enables the design of compact antenna arrays. We formulate the problem into a convex optimization to obtain the optimal load impedance for each antenna element. The numerical results show that the proposed schemes based on constructive interference can achieve significant performance gains over

conventional case with fixed mutual coupling, especially when the antenna spacing is small. Extensions to multi-user case will be a research focus in the future.

ACKNOWLEDGMENT

This work was supported by the Royal Academy of Engineering, UK, the Engineering and Physical Sciences Research Council (EPSRC) project EP/M014150/1, and the China Scholarship Council (CSC).

REFERENCES

[1] D. Gesbert, M. Shafi, D. S. Shiu, P. Smith, and A. Naguib, "From theory to practice: An overview of MIMO space-time coded wireless systems," *IEEE J. Sel. Areas Commun.*, vol. 21, no. 3, pp. 281-302, Apr. 2003.

[2] A. J. Paulraj, D. Gore, R. Nabar, and H. Bolcskei, "An overview of MIMO communications - A key to gigabit wireless," *Proceedings of IEEE*, vol. 92, no. 2, pp. 198-218, Feb. 2004.

[3] K. -K. Wong, and A. Paulraj, "On the decoding order of MIMO maximum-likelihood sphere decoder: linear and non-linear receivers," *Vehicular Technology Conference, 2004. VTC 2004-Spring. 2004 IEEE 59th*, vol. 2, pp. 698-702, May 2004.

[4] C. Wang, E. K. S. Au, R. D. Murch, W. H. Mow, R. S. Cheng, and V. Lau, "On the Performance of the MIMO Zero-Forcing Receiver in the Presence of Channel Estimation Error," *IEEE Trans. Wireless Commun.*, vol. 6, no. 3, pp. 805-810, Mar. 2007.

[5] M. R. McKay, I. B. Collings, and A. M. Tulino, "Achievable Sum Rate of MIMO MMSE Receivers: A General Analytical Framework," *IEEE Trans. Inf. Theory*, vol. 56, no. 1, pp. 396-410, Jan. 2010.

[6] A. Zanella, M. Chiani, and M. Z. Win, "MMSE Reception and Successive Interference Cancellation for MIMO Systems with High Spectral Efficiency," *IEEE Trans. Wireless. Commun.*, vol. 4, no. 3, pp. 1244-1253, May 2005.

[7] C. Masouros, M. Sellathurai, and T. Ratnarajah, "Large-Scale MIMO Transmitters in Fixed Physical Spaces: The Effect of Transmit Correlation and Mutual Coupling," *IEEE Trans. Commun.*, vol. 61, no. 7, pp. 2794-2804, July 2013.

[8] M. T. Ivrlac, W. Utschick, and J. A. Nossek, "Fading correlations in wireless MIMO communication systems," *IEEE J. Sel. Areas Commun.*, vol. 21, no. 5, pp. 819-828, June 2003.

[9] A. M. Sayeed, "Deconstructing multiantenna fading channels," *IEEE Trans. Sig. Process.*, vol. 50, no. 10, pp. 2563-2579, Oct. 2002.

[10] M. Steinbauer, A. Molisch, and E. Bonek, "The double-directional radio channel," *IEEE Ant. Propag. Mag.*, vol. 43, no. 4, pp. 51-63, Aug. 2001.

[11] A. Forenza, D. J. Love, and R. W. Heath, "Simplified Spatial Correlation Models for Clustered MIMO Channels with Different Array Configurations," *IEEE Trans. Veh. Tech.*, vol. 56, no. 4, pp. 1924-1934, July 2007.

[12] M. T. Ivrlac, W. Utschick, and J. A. Nossek, "Fading correlations in wireless MIMO communication systems," *IEEE J. Sel. Areas Commun.*, vol. 21, no. 5, pp. 819-828, June 2003.

[13] D. Piazza, N. J. Kirsch, A. Forenza, R. W. Heath, and K. R. Dandekar, "Design and evaluation of a reconfigurable antenna array for MIMO systems," *IEEE Trans. Ant. Propag.*, vol. 56, no. 3, pp. 869-881, Mar. 2008.

[14] P. L. Kafle, A. Intarapanich, A. B. Sesay, J. McRory, and R. J. Davies, "Spatial correlation and capacity measurements for wideband MIMO channels in indoor office environment," *IEEE Trans. Wireless Commun.*, vol. 7, no. 5, pp. 1560-1571, May 2008.

[15] A. M. Tulino, A. Lozano, and S. Verdu, "Impact of antenna correlation on the capacity of multiantenna channels," *IEEE Trans. Inf. Theory*, vol. 51, no. 7, pp. 2491-2509, July 2005.

[16] H. Liu, Y. Song, and R. C. Qiu, "The impact of fading correlation on the error performance of MIMO systems over Rayleigh fading channels," *IEEE Trans. Wireless Commun.*, vol. 4, no. 5, pp. 2014-2019, Sept. 2005.

[17] C.-K. Wen, Y.-N. Lee, J.-T. Chen, and P. Ting, "Asymptotic spectral efficiency of MIMO multiple-access wireless systems exploring only channel spatial correlations," *IEEE Trans. Sig. Process.*, vol. 53, no. 6, pp. 2059-2073, June 2005.

[18] A. Alexiou, and M. Qaddi, "Robust linear precoding to compensate for antenna correlation in orthogonal space-time block coded systems," in *Proc. 2004 Sensor Array and Multichannel Signal Processing Workshop*, pp. 701-705.

[19] H. R. Bahrami, and T. Le-Ngoc, "Precoder design based on the channel correlation matrices," *IEEE Trans. Wireless Commun.*, vol. 5, no. 12, pp. 3579-3587, Dec. 2006.

[20] J. Akhtar, and D. Gesbert, "Spatial multiplexing over correlated MIMO channels with a closed-form precoder," *IEEE Trans. Wireless Commun.*, vol. 4, no. 5, pp. 2400-2409, Sept. 2005.

[21] B. Clerckx, C. Craeye, D. V-Janvier, and C. Oestges, "Impact of Antenna Coupling on 2×2 MIMO Communications," *IEEE Trans. Veh. Tech.*, vol. 56, no. 3, pp. 1009-1018, May 2007.

[22] S. Lu, H. T. Hui, M. E. Bialkowski, X. Liu, H. S. Hui, and N. V. Shuley, "Effects of antenna coupling on the performance of MIMO systems," in *Proc. 29th Symposium on Information Theory*, pp. 2945-2948.

[23] C. A. Balanis, *Antenna Theory: Analysis and Design*, 3rd edition.

[24] I. Gupta, and A. Ksienski, "Effect of mutual coupling on the performance of adaptive arrays," *IEEE Trans. Ant. Propag.*, vol. 31, no. 5, pp. 785-791, Sept. 1983.

[25] A. A. Abouda, and S. G. Haggman, "Effect of mutual coupling on capacity of MIMO wireless channels in High SNR," *Progress in Electromagnetics Research*, vol. 65, pp. 27-40, 2005.

[26] H. Steyskal, and J. S. Herd, "Mutual coupling compensation in small array antennas," *IEEE Trans. Ant. Propag.*, vol. 38, no. 2, pp. 1971-1975, Dec. 1990.

[27] J. Corcoles, M. A. Gonzalez, and J. Rubio, "Mutual coupling compensation in arrays using a spherical wave expansion of the radiated field," *IEEE Ant. Wireless Propag. Lett.*, vol. 8, pp. 108-111, 2009.

[28] G. Moreno, H. M. Bernety, and A. B. Yakovlev, "Reduction of Mutual Coupling between Strip Dipole Antennas at Terahertz Frequencies with an Elliptically Shaped Graphene Monolayer," *IEEE Ant. Wireless. Propag. Lett.*, DOI: 10.1109/LAWP.2015.2505333, 2015.

[29] S. Farsi, H. Aliakbarian, D. Schreurs, B. Nauwelaers, and G. A. E. Vandenbosch, "Mutual Coupling Reduction Between Planar Antennas by Using a Simple Microstrip U-Section," *IEEE Ant. Wireless. Propag. Lett.*, vol. 11, pp. 1501-1503, 2012.

[30] Z. Li, Z. Du, M. Takahashi, K. Saito, and K. Ito, "Reducing Mutual Coupling of MIMO Antennas with Parasitic Elements for Mobile Terminals," *IEEE Trans. Ant. Propag.*, vol. 60, no. 2, pp. 473-481, Feb. 2012.

[31] H. T. Hui, "A practical approach to compensate for the mutual coupling effect in an adaptive dipole array," *IEEE Trans. Ant. Propag.*, vol. 52, no. 5, pp. 1262-1269, May 2004.

[32] I. Salonen, A. Toropainen, and P. Vainikainen, "Linear pattern correction in a small microstrip antenna array," *IEEE Trans. Ant. Propag.*, vol. 52, no. 2, pp. 578-586, Feb. 2004.

[33] R. S. Adve, and T. K. Sarkar, "Compensation for the effects of mutual coupling on direct data domain adaptive algorithm," *IEEE Trans. Ant. Propag.*, vol. 48, no. 1, pp. 86-94, Jan. 2000.

[34] C. Masouros, "Correlation Rotation Linear Precoding for MIMO Broadcast Communications," *IEEE Trans. Sig. Process.*, vol. 59, no. 1, pp. 252-262, Jan. 2011.

[35] C. Masouros, T. Ratnarajah, M. Sellathurai, C. Papadias, A. Shukla, "Known interference in the cellular downlink: a performance limiting factor or a source of green signal power? ," *IEEE Comms. Mag.*, vol. 51, no. 10, pp. 162-171, Oct. 2013.

[36] G. Zheng, I. Krikidis, C. Masouros, S. Timotheou, D. A. Toumpakaris, Z. Ding, "Rethinking the Role of Interference in Wireless Networks," *IEEE Comms. Mag.*, vol.52, no.11, pp.152,158, Nov. 2014.

[37] J. Choma, and W. K. Chen, *Feedback Networks: Theory and Circuit Applications*. U.S.A.: World Scientific Publishing, May 2007.

[38] H. A. Haus, *Electromagnetic Noise and Quantum Optical Measurements*. Springer, Nov. 2000.

[39] Jia-Shiang Fu, "Adaptive Impedance Matching Circuits Based on Ferroelectric and Semiconductor Varactors", *Ph.D. thesis*, University of Michigan, 2009.

[40] J. Lu, D. Ireland, and R. Schlub, "Dielectric Embedded ESPAR (DE-ESPAR) Antenna Array for Wireless Communications," *IEEE Trans. Ant. Propag.*, vol. 53, no. 8, pp. 2437-2443, Aug. 2005.

[41] E. P. Tsakalaki, O. N. Alrabadi, C. B. Papadias, and R. Prasad, "Adaptive reactance-controlled antenna systems for multi-input multi-output applications," *IET Microw. Antennas Propag.*, vol. 5, no. 8, pp. 975-984, 2011.

[42] O. N. Alrabadi, C. Divarathne, P. Tragas, A. Kalis, N. Marchetti, C. B. Papadias, and R. Prasad, "Spatial Multiplexing with a Single Radio: Proof-of-Concept Experiments in an Indoor Environment with a 2.6-GHz Prototype," *IEEE Commun. Lett.*, vol. 15, no. 2, pp. 178-180, Feb. 2011.